ISSN 2618-1584 Vol. 3, Issue 6: 52-63, DOI: 10.25236/FMSR.2021.030610

Movement Mechanisms and Numerical Simulation of Virus-containing Exhaled Droplets

Jiawen Han

Imperial College London, London, SW7 2BX

Abstract: *The problem of viral and microbial contamination has received extensive and high attention from scholars at home and abroad. A great deal of information and research has demonstrated that droplets containing organisms such as viruses and bacteria can be airborne, so it is extremely important to study the movement and transmission patterns of the particles. Human coughing and sneezing are the main sources of viral droplets and are the focus of this paper. This topic starts with a theoretical approach to investigate the propagation law of microbial aerosols in the air, combined with the characteristics of droplets, to establish a model of microbial particle dispersal. And based on the Lagrangian method, the model is simplified and the 4th order standard Runge-Kutta algorithm is used to numerically solve the differential equations based on the Matlab platform, so as to analyse the effects of factors such as jet velocity, ambient wind speed and the size of the exhaled virus particles occurring on the particle motion. The evaporation of particles also has a relatively large effect on the motion of smaller sized particles, which after complete evaporation will will float in the air and will no longer hit the ground. Ultimately, the analysis of particle movement distances leads to recommendations for the prevention of airborne infectious disease transmission.*

Keywords: *exhaled droplets, infectious disease transmission, Runge-Kutta method, contaminated area*

1. Introduction

When microbial particles below 10 microns are emitted from the human mouth, they will not settle quickly due to their small size and will remain suspended in the air with the flow of air, often staying in the air for a long time through primary dusting and secondary airflow. The larger droplets produced by sneezing or coughing can become droplet nuclei, or microorganisms with pathogens, due to their own evaporation, and these microorganisms are spread around in the air with the wind movement, leading to droplet transmission.

According to clinical studies by a number of academics, there are three routes of transmission of novel coronaviruses. One is contact transmission, which is transmission caused by direct or indirect contact of the pathogen through hands and vectors, such as droplets deposited on the surface of objects. The second is droplet transmission, which is transmission with droplet nuclei(>5 microns) referring to pathogenic microorganisms that move over short distances in the air(usually within 2 to 5 metres) to the mouth, nasal mucosa or conjunctiva of susceptible people, such as droplets from patients sneezing, coughing or talking. Airborne transmission, as the third mode of transmission, is the spread of disease(mainly aerosol transmission) by airborne micro-particles(65 microns) with pathogenic micro-organisms[1].

The horizontal distances that exhaled particles can reach vary with the three different modes of propagation above. The Centers for Disease Control recommends a safe outdoor socialization distance of about 6 feet(1.83 metre)[2]. The combined effect between gravity, inertial forces, drag and environmental forces determines the fate of saliva droplets. In this paper, the Runge-Kutta algorithm will be applied to predict the farthest distances that particles of different sizes can reach in air and to consider the effect of evaporation of droplets in air on their movement.

2. Comprehensive Force Analysis of Droplets Motion

The forces on aerosols moving in air are analysed in order to provide a basis for the study of microbial aerosol movement patterns. The wide variety of microbial aerosols presents a number of problems for force analysis. In order to simplify the analysis, the rigid spherical particles were analysed.

ISSN 2618-1584 Vol. 3, Issue 6: 52-63, DOI: 10.25236/FMSR.2021.030610

And we only consider the movement of droplets in space, not the rotation of droplets.

The droplet is exhaled from the mouth by a combination of the following eight forces: air resistance(Drag)[3] ($F_d = \frac{\pi d_p^2 \rho_a |u_a - u_p|(u_a - u_p) C_d}{8 C_c} \times \frac{1 + \frac{2\mu_a}{3\mu_p}}{1 + \frac{\mu_a}{\mu_p}}$), thermophoretic force[4]($F_{th} = -\frac{3\pi \mu_a^2 d_p H_{th}}{\rho_a T} \cdot \nabla T$), gravity and buoyancy(Fg = $m_p g = \frac{1}{6}\pi d_p^3 \rho_p g$ and $F_b = -\frac{1}{6}\pi d_p^3 \rho_a g$), added drag[5] ($F_m = \frac{1}{12}\rho_a \pi d_p^3 \left(\frac{du_a}{dt} - \frac{du_p}{dt}\right)$), Basset force[6](FB = $\frac{3}{2} d_p^2 \sqrt{\rho_a \mu_a \pi} \int_0^t \left(\frac{du_a}{d\tau} - \frac{du_p}{d\tau}\right) \cdot \frac{1}{\sqrt{t-\tau}} d\tau$), Saffman lift force[7]($F_S = 1.61 d_p^2 (\rho_a \mu_a)^{\frac{1}{2}} (u_a - u_p) \left|\frac{du_a}{dy}\right|^2$) and Brownian motion force[8]($F_{Bi} = \xi_i \cdot \sqrt{\frac{6\pi \mu_a \sigma T d_p}{C_c \triangle t}}$).

Here, d_p is the diameter of the sphere, u_a and u_p are the velocities of the surrounding air and the particle respectively, ρ_a is the air density, $C_d = C_{D_0} \cdot \frac{2\mu_a + 3\mu_p + k}{3\mu_a + 3\mu_p + k} \cdot h$ is the drag coefficient and it varies for different airflows and particle velocities, $C_c = 1 + \frac{2\lambda}{d_p}(1.257 + 0.4 \cdot e^{\frac{-0.55 d_p}{\lambda}})$ is the Cunningham correction factor[9], Re_p is the droplet Reynolds number, μ_a is the saturated vapour kinetic viscosity, μ_p is the droplet kinetic viscosity, k is the droplet internal loop flow rate and is taken as $k = 0$, h is the droplet deformation rate and is taken as $h = 1.5$ for $h \in (1,\infty)$, ∇T is the thermodynamic temperature gradient, H_{th} is the thermophoretic force coefficient, k_a, k_b are the coefficients of heat transfer between air and particles, $k_a = 0.242 W/(m \cdot K)$, $k_b = 0.0454 W/(m \cdot K)$, λ is the mean free path of air molecules, $\frac{du_a}{dy}$ is the ambient velocity gradient perpendicular to the direction of particle motion, ξ_i is an independent Gaussian probability distribution(normal distribution) random number with expectation zero and variance unit variance(in general, $-30 < \xi_i < 30$), and $4t$ is the time interval over which the random force acts.

Although the forces acting on a particle are quite complex, in general not all forces are equally important and it is possible to consider the main forces in the calculation and ignore the more minor ones, depending on the actual situation. The forces on the motion of microbial particles have been analysed above, and whether certain forces can be neglected when solving their motion problems depends to a large extent on the size of the particles and their density. The particles involved in this study are mainly concentrated in the $0.1 - 200 \mu m$ range. In this paper the various possible forces are calculated and their orders of magnitude are discussed based on the following assumptions in order to determine the main forces:

1) The coronavirus(SARS-CoV-2) and the cough droplet containing the microbial particle is considered to have a diameter of 10 microns[10] and a particle density of $993 kg/m^3$ at 36.5 degrees Celsius and an air density of $1.184 kg/m^3$.

2) The thermodynamic temperature is: $T = 273.15 + t(^\circ C) = 273.15 + 20 = 293.15 K$ when $t = 20^\circ C$.

3) To simplify the arithmetic, assume that the initial velocity of the coughing droplets is $28 m/s$ and the ambient wind speed is $0.4 m/s$, both of which are horizontal. The aerodynamic and droplet dynamic viscosities are $17.9 \times 10^{-6} N \cdot s/m^2$ and $7.2 \times 10^{-4} N \cdot s/m^2$ respectively.

The magnitudes of the forces on the particles, as calculated by the above seven forces respectively, are shown in the table 1.

Table 1: Summary of the order of magnitude of the various forces on moving particles.

Forces	F_d	F_{th}	F_g	F_b	F_m	F_B	F_S	F_{Bi}
Order of Magnitude(*N*)	10^{-8}	10^{-17}	10^{-12}	10^{-15}	10^{-17}	$<10^{-12}$	$< 10^{-11}$	10^{-15}

From the above results it can be seen that for the problem of microbial aerosol motion, the magnitude of the various forces on them is not the same. The effect of the thermophoretic force on the particles is negligible compared to the gravitational and drag forces, so we will not consider the effect of this force in the subsequent numerical calculations.

3. Evaporation Nucleation

The force analysis shows that the trajectory of the particles is very complex. Also the movement of

ISSN 2618-1584 Vol. 3, Issue 6: 52-63, DOI: 10.25236/FMSR.2021.030610

microbial particles is accompanied by physical phenomena such as evaporation, sedimentation and diffusion. In this section evaporation during droplet movement will be analysed.

The size distribution and quantity of droplets has been studied since the 1940s. Duguid[11] found that the size of the droplets from talking, coughing and sneezing ranged from 1 to 2000 μm, and 95% of the droplets were between 2 and 100 μm in size. Also, the geometric particle size distribution of droplet nuclei ranged from 0.25 to 42 μm, with approximately 97% in the range of 0.5 to 12 μm and most commonly in the range of 1 to 2 μm.

In 1918, Langmuir proposed an equation[12] to calculate the evaporation problem as:

$$\frac{dd_p}{dt} = \frac{4DM}{Rd_p\rho_p}\left(\frac{p_\infty}{T_\infty} - \frac{p_d}{T_d}\right). \tag{1}$$

Here D is the diffusion coefficient, ρ is the vapour density of the evaporated substance, p_∞ is the partial pressure of the vapour away from the droplet, p_d is the vapour pressure at the surface of the particle, M is the molecular weight, R = 8.3145$J/(K \cdot mol)$ is the gas constant, and T_∞ and T_d are the ambient and droplet surface (thermodynamic) temperatures respectively. Using the above equation we can calculate the time it takes for a droplet of diameter d_1 to evaporate to d_2($d_1 > d_2$):

$$t = \frac{R\rho_p}{8DM} \cdot (d_2^2 - d_1^2)\left(\frac{p_\infty}{T_\infty} - \frac{p_d}{T_d}\right)^{-1}. \tag{2}$$

For example, an exhaled droplet with a size of 100 μm is emitted from the mouth at 37$^\circ C$ to 20$^\circ C$. Assuming that the molar mass of the droplets is the same as that of water($M = 18 \times 10^{-3} kg/mol$), the mass diffusivity is 0.282cm/s^2 and the saturated vapor pressure is p_d = 6.2795kPa and p_∞ = 2.3388kPa respectively. Then, when d_2 = 0, the lifetime of the droplet is 1.66s for a 100 μm droplet to evaporate completely in air.

4. Prediction of Microbial Aerosol Movement

The simulation and prediction of the distribution of exhaled viral microorganisms in air is one of the important application areas of computational fluid dynamics(CFD) methods. It is common practice to first simulate the turbulent flow of the environment and then to predict the spatial distribution of viral microbial droplets based on the flow field distribution obtained from the solution. The two commonly used methods are the Eulerian and Lagrangian methods, and the division between the two methods is based on the different types of reference units in the simulation.

In the Eulerian model, the reference unit is considered to be static and the particulate matter passes through a fixed control volume in a continuous state. Numerous previous studies[13] have shown that the use of the Eulerian method introduces numerical diffusion problems, which can seriously affect the accuracy of the results and simulations. The Lagrangian model requires the assumption that the air is in continuous phase. It enables a more accurate description of the motion of sparse particles in the gas stream by calculating the trajectory of the particles, it allows the interphase coupling between the continuous and discrete phases to be considered simultaneously and the effect of the coupling on the discrete phase orbit and the continuous phase flow. The basic idea is to assume that the particles under study are rigid bodies, to analyse the forces on individual particles in the flow field and to establish equations of motion for them in the form of Newton's second law, integrating twice to obtain the trajectories of the particles.

Based on the results of the above analysis, we would ignore the coupling problem between the gas and liquid, and also ignore the collisional adhesion phenomenon between the particles. Then, based on Newton's second law and the analysis in Subsection2.1, the equation of motion for a single particle can be given as

$$m_p\frac{d\vec{V_p}}{dt} = \sum F = F_d + F_g + F_b + F_m + F_B + F_S + F_{Bi}, \tag{3}$$

where $\tilde{V_p}$ is the initial velocity vector of the particle in three dimensions.

Bringing each force into the above equation and $\tilde{V}$ = (u,v,w) and $\tilde{V_p}$ = (u_p,v_p,w_p) where $\tilde{V}$ is the ambient wind speed. We have:

ISSN 2618-1584 Vol. 3, Issue 6: 52-63, DOI: 10.25236/FMSR.2021.030610

$$\frac{du_p}{dt} = F_{d_x} + F_{m_x} + F_{Bi} + F_{B_x}, \tag{4}$$

$$\frac{dv_p}{dt} = F_{d_y} + F_{m_y} + F_{Bi} + F_{B_y}, \tag{5}$$

$$\frac{dw_p}{dt} = F_g + F_b + F_{d_z} + F_{m_z} + F_{Bi} + F_{B_z} + F_S \tag{6}$$

These three equations involve three unknown functions, the velocity components u_p, v_p and w_p. The corresponding coordinate system is oriented with the x-direction parallel to the ground and the initial velocity of the droplet having a partial velocity in the x-direction, the z-direction perpendicular to the ground and downwards, and the y-direction perpendicular to the x-direction and parallel to the ground. The displacement of a droplet particle can be obtained by integrating its velocity fuction. The drag coefficient C_d inside the drag force is related to the Reynolds number $Re_p = \frac{d_p|u-u_p|\rho_a}{\mu_a}$, which in turn is related to the velocity. It is evident that the differential equation for the motion of a droplet in air is complex and difficult to integrate directly to obtain an analytical solution. Numerical methods are usually used to calculate the differential equations.

4.1 Runge-Kutta Method

The initial value problem for a first order ordinary differential equation can be written simply as: $y^0 = f(x,y)$, $x_0 = a$ 6 x 6 b and $y(x_0) = y_0$. The so-called numerical solution method seeks an approximation $y_i(i = 1,2,...,n)$ to the value $y(x_i)$ of the solution of the equation(4) over a series of discrete nodes. The distance $h_i = x_i - x_{i-1}$ between two adjacent nodes is called the step from node x_{i-1} to node x_i. The steps $h_i(i = 1,2,...,n)$ can be equal or unequal.

The fourth-order Runge-Kutta format with fourth-order accuracy is used as the main method for numerical calculations in this paper. The initial iteration values, that is the initial displacement and initial velocity of the droplets and the ambient wind speed, needed to be determined prior to solving. The step size of the iterative process(h) and the time span of the droplets also need to be determined. The specific equations for the fourth-order Runge-Kutta method are:

$$\begin{cases} k_{i1} = f_i(t_j, y_{1j}, y_{2j}, ..., y_{nj}), \\ k_{i2} = f_i\left(t_j + \frac{h}{2}, y_{1j} + \frac{hk_{11}}{2}, ..., y_{nj} + \frac{hk_{n1}}{2}\right) \\ k_{i3} = f_i\left(t_j + \frac{h}{2}, y_{1j} + \frac{hk_{12}}{2}, ..., y_{nj} + \frac{hk_{n2}}{2}\right), \\ k_{i4} = f_i(t_j + h, y_{1j} + hk_{13}, ..., y_{nj} + hk_{n3}), \\ y_{i,j+1} = y_{i,j} + \frac{h}{6}(k_{i1} + 2k_{i2} + 2k_{i3} + k_{i4}), \\ i = 1, 2, ..., n, \end{cases} \tag{7}$$

where i is the equation entry in the set of differential equations and j is the current time step.

4.2 Numerical Setup

4.2.1 Cough and Sneeze Particles Size and Velocity Distribution

Experimental results[10] showed that infected individual exhales sneezing particles with a double-peaked geometric mean size[14], 386.2 μm and 72 μm, respectively. Kwon[15] concluded that the average initial coughing velocity was 15.3m/s for the males studied and 10.6m/s for the females. However, the maximum velocity of the exhaled airflow of sneeze is around 30–100m/s, significantly larger than that of cough, breath and speech[14]. Futhermore, Kwon[15] measured the initial velocity of the exhaled airflow when 26 subjects coughed and spoke using Particle Image Velocimetry(PIV) and analysed it to obtain the angle of the exhaled airflow. The results indicated that the angle of the coughed air is roughly 38° for males and 32° for females.

4.2.2 Parameter Selection in the Runge-Kutta Method

We set the time span to one second, within which the exhaled particles will finish settling. At the same time the number of steps in the Runge-Kutta method is set to 10000 in order to increase the accuracy of the calculation. The code also uses the ”feval” function to execute the Runge-Kutta function and the corresponding arguments, and allows the function to accept any number of input

ISSN 2618-1584 Vol. 3, Issue 6: 52-63, DOI: 10.25236/FMSR.2021.030610

arguments(adding the input variable "varargin").

4.2.3 Variation of Ambient Wind Speed with Height

Since exhaled particles are only active about 2*m* above the ground, we have made the ambient wind speed gradient in the z-direction the focus of attention, while the x and y-directions are considered constants. Wind speed increases with height, with wind speeds near the earth's surface being slowed down by obstacles such as trees. The hourly average wind vector (speed and direction) ten metres above the ground in London over the course of a year is approximately 16*km/h*[16]. Then, the variation of wind speed with height can be written as[17]:

$$w = 0.44 \left(\frac{h_2}{10} \right)^{0.2}. \tag{8}$$

where w and w_0 are the measured wind speeds at elevations h_2 and h_1 respectively, and $\alpha = 0.2$ is the wind shear coefficient.

4.2.4 Displacement of Particles

We use the trapezoidal rule for integration to calculate the displacement of exhaled droplets:

$$\int_0^{N\triangle t} u_p dt \approx \sum_{k=1}^{N} \frac{u_p(t_{k-1}) + u_p(t_k)}{2} \cdot \triangle t,$$

where u_p is the velocity of droplets and N is the number of steps.

4.2.5 Approximation of Basset Force

The integral term involved in the Basset force can be approximated by finite differentiating the velocity vectors of the particles and then summing them(discretizing):

$$\int_0^t \left(0 - \frac{d\vec{V_p}}{d\tau} \right) \cdot \frac{1}{\sqrt{t-\tau}} d\tau = -\sum_{n=0}^{N-1} \frac{1}{\sqrt{t-n\triangle t}} \cdot \frac{\vec{V_p}((n+1)\triangle t) - \vec{V_p}(n\triangle t)}{\triangle t} \cdot \triangle t. \tag{9}$$

Here $t = N4t$. If the difference of the values of the point t,t+4t is taken as an approximation of the derivative where 4t is the time step, then:

$$\vec{V_p}(t+\triangle t) = \vec{V_p}(t) + \vec{V_p}'(t) \cdot \triangle t + o(\triangle t) \Longrightarrow \left| \vec{V_p}'(t) - \frac{\vec{V_p}(t+\triangle t) - \vec{V_p}(t)}{\triangle t} \right| = o(1) \tag{10}$$

The error after the approximation is therefore infinitesimal.

4.3 Results and Discussion

We used initial parameters, i.e. initial particle($\vec{V_p}$) and environmental(V~) velocities, and initial size distributions(d_p) to simulate the dynamic mechanisms of exhalated droplets, and this was based on reports in the experimental literature.

4.3.1 Results Without Considering the Evaporation Effect

First, we consider the trajectory of a sneezing droplet with a diameter of 380 μm through the air. The microbial aerosol is dispersed at a speed of 30*m/s* (an angle of 38° to the x-direction). The source at the point of dispersal is 1.8*m* above the ground. The ambient outdoor wind speed is horizontally uniform and stable with a magnitude of 0.4*m/s* and vertically satisfies equation(8).

Figure 1 and Figure 2 show the velocity change along the x-direction of the sneeze droplet after it has been erupted from the mouth and the trajectory of its movement. It can be seen that for particles with a diameter of 380 μm, the particles are able to maintain a large velocity in the x-direction due to their own inertia. The velocity of the droplet decreases rapidly in the 0.2*s* time period after it is ejected, then reaches the ambient wind speed at 0.4*s* and continues to propagate, eventually landing at a velocity of 0 at approximately 0.7*s*.

From Figure 2, the 380 μm particle travels a distance of at least 1.5*m*.

ISSN 2618-1584 Vol. 3, Issue 6: 52-63, DOI: 10.25236/FMSR.2021.030610

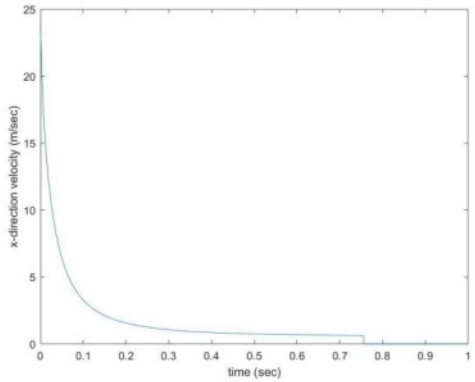

Figure 1: x-velocity vs. time(380μm)

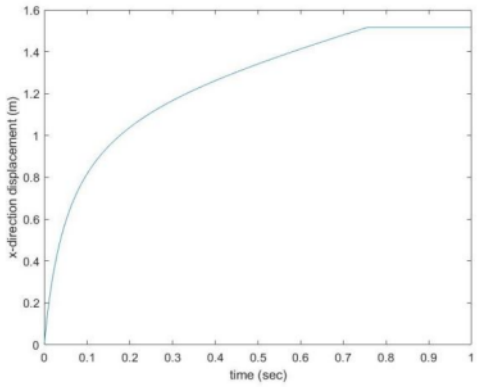

Figure 2: x-displacement vs. time(380μm)

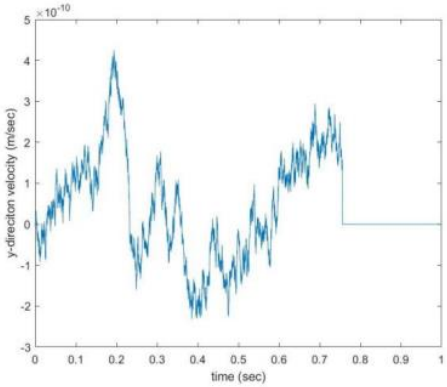

Figure 3: y-velocity vs. time(380μm)

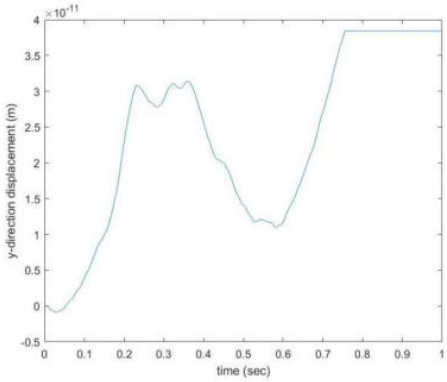

Figure 4: y-displacement vs. time(380μm)

ISSN 2618-1584 Vol. 3, Issue 6: 52-63, DOI: 10.25236/FMSR.2021.030610

Figure 3 and Figure 4 show the change in velocity in the y-direction as well as the trajectory of the motion. The ambient wind speed in the y-direction is 0m/s and the initial velocity of the droplet in the y direction is also 0m/s. The velocity variation of the motion caused by the force on the sneezing particles is shown in Figure 3, with the velocity fluctuating up and down in the interval $(-2 \times 10^{-10} m/s, 4 \times 10^{-10} m/s)$.

The trajectory diagram of the motion(Figure 4) shows that the particle motion also fluctuates around the mouth and for this diagram up to $3.7 \times 10^{-11} m$. Since there is a directional force without specifying positive or negative, the particle may move symmetrically along the positive and negative axes for the y-direction. The $380\mu m$ particle itself has a very high inertia in the x-direction and therefore acquires a much smaller velocity and travels a much smaller distance in the y-direction than in the x-direction.

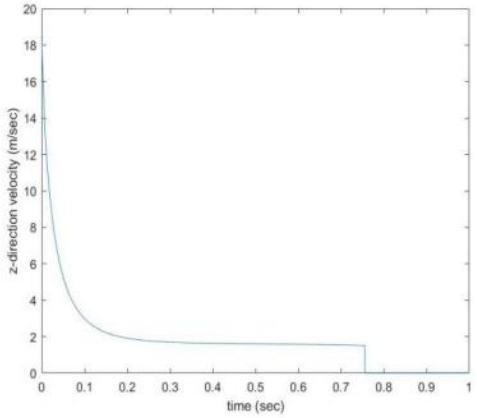

Figure 5: z-velocity vs. time(380 μm)

Figure 5 and Figure 6 describe the velocity variation of the droplet in the z-direction and the trajectory of the motion. The ambient wind speed in the z-direction varies with height(equation(4.6)), while there is also a component velocity of the particle in the z-direction.

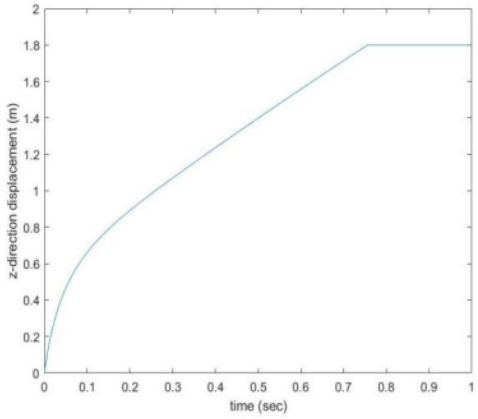

Figure 6: z-displacement vs. time(380 μm)

In Figure 6, the particle velocity drops rapidly over 0.1s and then coincides with the ambient wind speed until it hits the ground at approximately 0.7s. Figure 6 is consistent with the trend in Figure 2 and is related to the presence of initial velocities in both the x and z-directions.

Observing Figure 7, the particle is mainly affected by inertia at first, and the displacement in the horizontal direction(x) is greater than that in the vertical direction(z). After around 0.4s, it is mainly affected by the ambient wind speed and sink with the air flow to the ground.

ISSN 2618-1584 Vol. 3, Issue 6: 52-63, DOI: 10.25236/FMSR.2021.030610

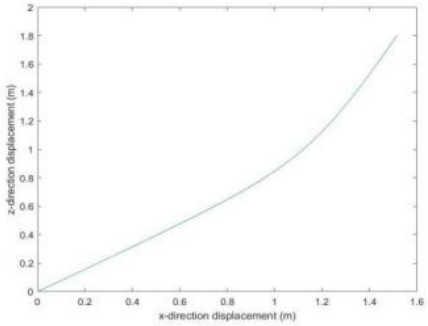

Figure 7: Displacement variations in the x and z-directions(380 μm)

Next, we look at the effect of different droplet diameters, different jet angles and different initial velocities on the trajectory of the particles. As coughing/sneezing is instantaneous, consider the furthest distance a particle can reach in 1 second.

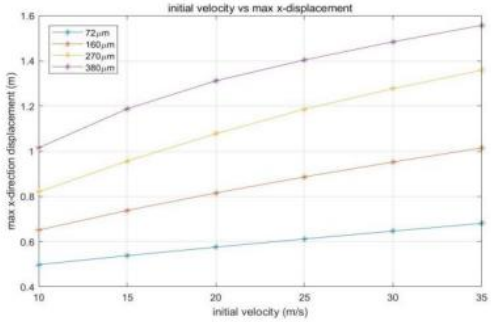

Figure 8: The maximum contamination distances in distances in 1 second for a range of particles diameters and initial velocities.

Figure 8 above compares the range of initial velocities from 10*m/s* to 35*m/s* and the horizontal maximum distances(contamination distances) for different droplet diameters(d_p = 72-380 μm). The horizontally maximum distance in 1 second of the sneezing droplet reach almost 1.57*m*, at the initial $V\sim_p$ = 35*m/s* and d_p = 380 μm. At the normal sneeze velocities $V\tilde{}_p$ = 10*m/s* , the maximum diaplacement for the average size of d_p = 160 μm is only 0.65*m*. It is clear that the size of the particles and the initial velocity of the eruption play an important role in the maximum contamination distance of the microdroplets. The figure shows that larger droplets carry more viruses and make the potential risk of airborne disease higher, and at moderate sneeze output the particles will reach a safe social distance of up to 2*m*. It is conceivable that under more violent conditions the exhaled particles would reach distances of up to 2 metres away.

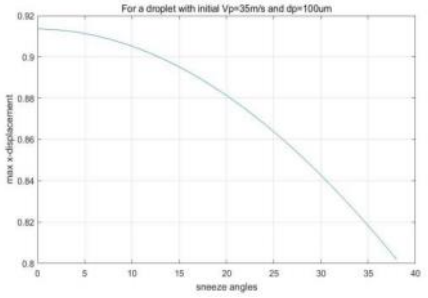

Figure 9: A specific sneeze with various jet angles.

Figure 9 above illustrates the change of maximum distance in 1 second for a particular sneeze with different jet angles(θ = 0°-38°). By increasing the jet angle, the infection distance was significantly reduced. At sneeze jet angles of 0° and 38°, the maximum distance reached by particles decreases from 0.913*m* to 0.8*m*, a decrease of about 14%. Therefore, it is recommended that people bend their heads when sneezing to avoid the spread of respiratory diseases such as coronaviruses.

ISSN 2618-1584 Vol. 3, Issue 6: 52-63, DOI: 10.25236/FMSR.2021.030610

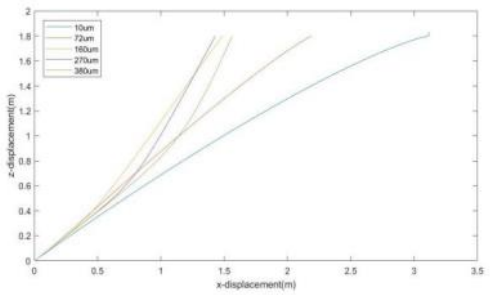

Figure 10: Droplets trajectory with the same initial velocity(35m/s) and jet angle(38◦).

For a long enough time, Figure 10 shows the longest distances that particles of different sizes can reach in the horizontal direction. For a particle of 10μm in size, its motion is characterised mainly by airflow following, while the effect of its own gravity and inertia is not apparent. It can reach up to 3m beyond the mouth. For droplets with a diameter of 72μm the settling problem is not negligible and the airflow following is not as pronounced as for 10μm, but is generally a combination of airflow following and gravitational settling, and the inertia is not very pronounced. Particles with diameters of 160μm,270μm and 380μm are mainly influenced by gravity and reach the ground very quickly. The trajectories in the diagram can be divided into three categories, with particles larger than 160μm apparently travelling shorter distances in the x-direction, similar to a parabola. The 72μm particle travelled comparable distances in the x and z-direction. The smaller particles(10μm) follow the wind horizontally over even twice the distance of the larger particles, resembling a power function curve with an exponent of less than 1.

4.3.2 Results Considering the Evaporation Effect

All of the above arguments do not take into account the evaporation of particles, however the volatilisation of particles during motion is not negligible. Equation(1) in Section3 can be added to our model, since most of the droplets ejected by sneezing are larger than 1μm.

When evaporation is not taken into account, small particles will eventually fall to the ground under sufficiently long time(the 10μm particles in Figure 10). But evaporation causes the droplets to become smaller and smaller to the point where they completely change into viral microorganisms in the range of approximately 0.02-0.3μm in diameter, and at this point such small particles will float in the air and their trajectories will eventually float in a certain area.

At the moment of sneezing, the real trajectory(considering evaporation and the values of the parameters are the same as in example in Section3.) of the particles will be of three types, as illustrated by the Figure 11.

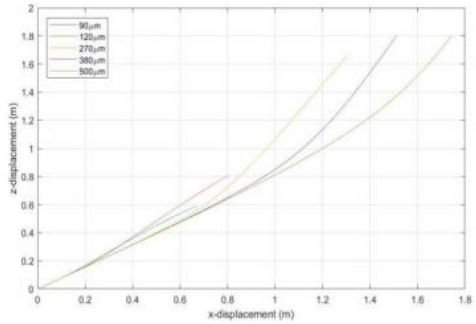

Figure 11: Trajectories of the droplets at five different initial diameter considering the evaporation effect(initial $\vec{V_p} = 30m/s$ *and* $\theta = 38^{\circ}$*).*

For small particles of 90 and 120μm diameter, they float at a height of 1-1.2m above the ground; for particles of 270μm, evaporation affects their settling, but they eventually fail to hit the ground and will float at a height of around 0.2m above the ground; and for particles of 380 and 500μm, they hit the ground before complete evaporation.

Using this model, we can study the effect of weather conditions on the evaporation and movement of sneeze droplets. Measurements of indoor and outdoor temperature changes were obtained after

ISSN 2618-1584 Vol. 3, Issue 6: 52-63, DOI: 10.25236/FMSR.2021.030610

measurements by Frank[18]. Table 2 shows the median indoor and outdoor temperatures and corresponding pressures in summer and winter.

Table 2: Seasonal variation in the temperature and relative pressure of indoor and outdoor conditions.

Temperature and Pressure	Summer	Winter
Outdoor	$T_\infty = 20^\circ C$, $p_\infty = 2.3388 kPa$	$T_\infty = 1^\circ C$, $p_\infty = 0.6572 kPa$
Indoor	$T_\infty = 24^\circ C$, $p_\infty = 2.9850 kPa$	$T_\infty = 19^\circ C$, $p_\infty = 2.1978 kPa$

The vertical time in Figure 12 is taken as the minimum of the time it takes for the particles(initial velocity is 35*m/s*) to evaporate completely and settle to the ground. It can also be interpreted that the left side of the curves is the time when the particle has completely evaporated and has not fallen to the ground(it will eventually continue to float in the air), while the right side is the time when the particle has fallen to the ground but has not completely evaporated.

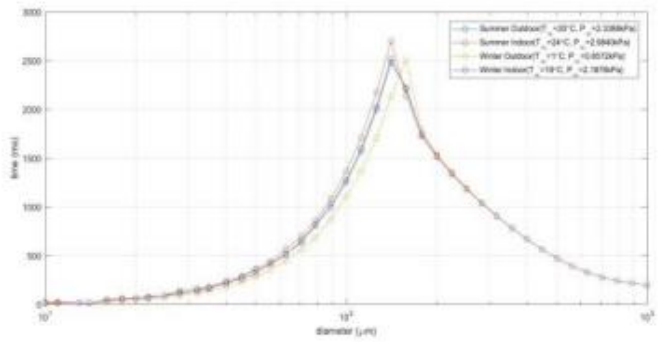

Figure 12: Evaporation-falling times for summer and winter.

All of four temperatures and pressures lead to a large fluctuation in the curves: particles with an initial diameter in the 50-150μm range will take longer to either evaporate completely or settle. This conclusion is inconsistent with the conclusion in the article written by Hongping Wang[3]. He concludes that the time for particle evaporation is much greater in winter outdoors than in the other three cases. The reason for this discrepancy is due to the fact that the equation(1) applied to our model does not include a parameter for the humidity of air, however Hongping elaborates that the humidity outdoors in winter is greater than the other three cases, which ultimately leads to a lower rate of particle evaporation. However, it is the same that for particles in the size range of 50-150μm, both Hongping and our model obtain evaporation times that are greater than those for particles of other sizes.

5. Conclusion

The main objective of this thesis is to numerically analyse the transport mechanisms and associated fluid dynamics of exhaled droplets produced by coughing/sneezing in an airborne environment. The forces that may be applied to the aerosol particles after they have been dispersed in the air are analysed in turn, and the magnitudes of each force are calculated, taking into account the virus-carrying droplets in the air that are the focus of this paper, and the forces that have a smaller effect are omitted after comparison, thus easing the burden for the subsequent numerical calculations. Next, evaporation and diffusion of microbial aerosols are also influencing their settling, and the time taken for particles of different sizes to evaporate into nuclei in air is calculated. Based on the data obtained from the experiments, we then applied the Runge-Kutta method to solve for the displacement that can be reached horizontally by the particles at different initial velocities, diameters and jet angles, i.e. the contaminated area. Then, the evaporation effect is added in particle movement model, giving a more realistic result.

We have found the following remarkable findings:

1) The evaporation of a droplet containing a virus ejected from the mouth is very rapid. For example, it takes 1.66*s* for a 100μm particle to evaporate completely, and if it is exhaled as a sneeze from 1.8*m* at an initial velocity of 30*m/s*, it has not yet hit the ground but has begun to follow the ambient wind speed until it hits the ground at roughly 3*s*.

2) Larger saliva droplets($d_p > 200\mu m$) are more influenced by gravity, inertial force and drag force.

ISSN 2618-1584 Vol. 3, Issue 6: 52-63, DOI: 10.25236/FMSR.2021.030610

In contrast, the effect of gravitational and inertial forces on small saliva droplets ($d_p > 50\,\mu m$) is negligible compared to the effect of the surrounding airflow.

3) A droplet with an average size of $d_p = 160\,\mu m$ is exhaled as a sneeze at $30 m/s$, causing it to be transported over a distance of around $1m$ in an instant (1 second). However, larger droplets with $d_p = 380\,\mu m$ have longer horizontal distances, being able to exceed $1.5m$.

4) Evaluation of different exhaled jet angles found that head bending as a protective measure reduced the maximum distance of droplet levels by more than 14%.

5) With sufficient time, a social distance of $2m$ may not be sufficient(up to $3.2m$ horizontally for $10\,\mu m$ droplets) as it relates to the ambient wind speed. A social distance of around $4m$ should be safer.

6) The evaporation of particles can also affect their trajectory. For small particles(0-$150\,\mu m$) evaporation dominates and it will float in the higher regions(1-$1.2m$); for medium sized particles(150-$300\,\mu m$) it takes longer to evaporate but eventually fails to hit the ground and will float at heights around $0.5m$; for larger particles(300-$1000\,\mu m$) evaporation has little effect on their settling.

7) When considering the effect of droplet evaporation on movement, a socially safe distance of $2m$ is valid for moderate sneeze eruptions up to $500\,\mu m$ at the moment of the eruption.

Certainly, in addition to the variables discussed in this article regarding the exhaled droplets themselves, ambient wind speed, distance between people, and whether or not the sick or susceptible person is wearing a mask all influence the spread of infectious diseases. A more reliable and safe social distance requires consideration of all these factors.

References

[1] Mark Nicas, William W Nazaroff, and Alan Hubbard. Toward understanding the risk of secondary airborne infection: emission of respirable pathogens. Journal of occupational and environmental hygiene, 2(3):143– 154, 2005.

[2] How to protect yourself and others. Website, 2021. https://www.cdc.gov/coronavirus/2019-ncov/prevent-getting-sick/prevention.html#stay6ft%20.

[3] Hongping Wang, Zhaobin Li, Xinlei Zhang, Lixing Zhu, Yi Liu, and Shizhao Wang. The motion of respiratory droplets produced by coughing. Physics of Fluids, 32(12):125102, 2020.

[4] LRKRWDR Talbot, RK Cheng, RW Schefer, and DR Willis. Thermophoresis of particles in a heated boundary layer. Journal of fluid mechanics, 101(4):737–758, 1980.

[5] CE Brennen. A review of added mass and fluid inertial forces. 1982.

[6] F Candelier, JR Angilella, and M Souhar. On the effect of the boussinesq–basset force on the radial migration of a stokes particle in a vortex. Physics of Fluids, 16(5):1765–1776, 2004.

[7] PGT Saffman. The lift on a small sphere in a slow shear flow. Journal of fluid mechanics, 22(2):385–400,1965.

[8] Efstathios E Michaelides. Brownian movement and thermophoresis of nanoparticles in liquids. International Journal of Heat and Mass Transfer, 81:179–187, 2015.

[9] CN Davies. Definitive equations for the fluid resistance of spheres. Proceedings of the Physical Society,57(4):259, 1945.

[10] Shinhao Yang, Grace WM Lee, Cheng-Min Chen, Chih-Cheng Wu, and Kuo-Pin Yu. The size and concentration of droplets generated by coughing in human subjects. Journal of Aerosol Medicine, 20(4):484–494, 2007.

[11] JP Duguid. The size and the duration of air-carriage of respiratory droplets and droplet-nuclei. Epidemiology & Infection, 44(6):471–479, 1946.

[12] Irving Langmuir. The evaporation of small spheres. Physical review, 12(5):368, 1918.

[13] Soon-Bark Kwon, Jaehyung Park, Jaeyoun Jang, Youngmin Cho, Duck-Shin Park, Changsoo Kim, GwiNam Bae, and Am Jang. Study on the initial velocity distribution of exhaled air from coughing and speaking. Chemosphere, 87(11):1260–1264, 2012.

[14] Climate and average weather year round in london. Website, 2021. https://weatherspark.com/y/45062/

[15] Shafiqur Rehman and Naif M Al-Abbadi. Wind shear coefficients and their effect on energy production. Energy Conversion and Management, 46(15-16):2578–2591, 2005.

[16] Mika Frankel, Gabriel Bek ̈o, Michael Timm, Sine Gustavsen, Erik Wind Hansen, and Anne Mette Madsen. Seasonal variations of indoor microbial exposures and their relation to temperature, relative humidity, and air exchange rate. Applied and environmental microbiology, 78(23):8289–8297, 2012.

ISSN 2618-1584 Vol. 3, Issue 6: 52-63, DOI: 10.25236/FMSR.2021.030610

[17] Sture Holmberg and Yuguo Li. Modelling of the indoor environment–particle dispersion and deposition. Indoor air, 8(2):113–122, 1998.
[18] ZY Han, WG Weng, and QY Huang. Characterizations of particle size distribution of the droplets exhaled by sneeze. Journal of the Royal Society Interface, 10(88):20130560, 2013.
[19] Wind shear. Website, 2021. https://www.engineeringtoolbox.com/wind-shear-d_1215.html.